A numerical prediction of bed shear stresses in the wave-current turbulent boundary layer over flat sea beds

Turbulent boundary layer
Wave-current interaction
Bed shear stress
Numerical modelling
Parameterization

Couche limite turbulente
Interaction houle-courant
Contrainte de cisaillement au fond
Modélisation numérique
Paramétrisation.

Son HUYNH-THANH[a] and André TEMPERVILLE[b]

[a] Faculty of Civil Engineering, Polytechnic Institute of Ho Chi Minh City, 268 Av. Ly Thuong Kiet, Q. 10, Ho Chi Minh City, Vietnam.

[b] Laboratoire des Ecoulements Géophysiques et Industriels, Institut de Mécanique de Grenoble, BP 53 X, 38041 Grenoble Cedex, France.

Received 28/10/93, in revised form 1/03/94, accepted 17/11/94.

ABSTRACT

The turbulent boundary-layer flow over flat rough beds due to a wave or to combined wave-current interaction is studied using a numerical turbulence closure model of K-L type. Different cases of modelling are discussed and illustrated by numerical examples. The model was run for a wide range of parameters of wave, current, bed roughness and angle of interaction. The curves of dimensionless mean and maximum bed shear stresses obtained present the non-linearity of the wave-current interaction. The parameterization of results is realized in order to facilitate the incorporation of bed shear stresses into coastal morphodynamic models.

RÉSUMÉ

Contraintes de cisaillement dans la couche limite turbulente sous l'interaction houle-courant.

La couche limite turbulente engendrée par la houle ou par l'interaction houle-courant est étudiée en utilisant un modèle numérique de fermeture turbulente du type K-L. Les différents cas de modélisation sont discutés et illustrés à travers des exemples numériques. L'exploitation du modèle pour une gamme importante des paramètres de la houle, du courant, de la rugosité du fond et de l'angle d'interaction est effectuée. Les courbes adimensionnelles représentant les contraintes de cisaillement moyenne et maximale obtenues avec le modèle montrent l'importance de la non-linéarité du problème. La paramétrisation des résultats est faite afin de faciliter l'incorporation des contraintes de cisaillement dans les modèles de morphodynamique côtière.

Oceanologica Acta, 1995, **18**, 1, 19-27.

INTRODUCTION

One of the important problems of coastal engineering is to study the oscillatory turbulent boundary layer near the sea bed, in which the shear stresses are important, permitting the movement of sediments. Under the force of waves, currents or wave-current combinations, the bed can be flat or rippled and sediments can be transported by rolling or suspension. Studies of the turbulent boundary layer generated by a sinusoidal wave or a wave-current interaction are not recent. A complete review can be found in Sleath (1989), Davies (1990) or Huynh-Thanh and Temperville (1990b, 1990c).

A detailed study of the turbulent bed boundary layer generated by combined wave-current flow, with a one-equation model, has been presented by Davies (1990). In this paper,

we concentrate on investigating the non-linearity effect of the wave-current interaction in the boundary layer over a flat sea bed using the turbulence closure model of K-L type developed in Huynh-Thanh and Temperville (1990b, 1990c). After the model formulation and the numerical method, a short presentation for the cases of a current alone and a wave alone will be given. We shall discuss the different types of modelling in the case of wave-current interaction through numerical examples. We devote special attention to the upper, boudary conditions. Some results which are obtained by running the model for various parameters of wave, current, bed roughness and angle of interaction will be presented. These results are then parameterized in the form of algebraic functions.

MODEL FORMULATION AND NUMERICAL METHOD

In the system of Cartesian coordinates (x, y, z) (Fig. 1), the current is supposed to flow in the x-direction and the wave is supposed to propagate in a direction which makes an angle f with the x-axis. We only consider here the case of a rough bed, hence the flat horizontal bottom is fixed at $z = z_0 = k_N/30$, where k_N represents the equivalent Nikuradse roughness. The value of k_N can be estimated by using empirical formulas such as $k_N = 2\ d_{90}$ (Kamphuis, 1975), where d_{90} is the diameter of particles in excess of 10 % of the weight of a grain sample. The still water depth is equal to h.

The system of equations is established with the following assumptions: (i) the thickness of the boundary layer is much smaller than the wavelength of the wave, (ii) the amplitude of the wave velocity $\hat{U}_h$ and of the mean current U_c is much smaller than the wave celerity C and (iii) the turbulence is fully developed on the total depth of the flow. Under these assumptions, the two horizontal components of velocity u and v (along x and y, respectively) are governed by the two linearized momentum equations:

$$\frac{\partial u}{\partial t} = -\frac{1}{\rho}\frac{\partial P}{\partial x} + \frac{\partial}{\partial z}\left(-\overline{u'w'}\right) \tag{1}$$

$$\frac{\partial v}{\partial t} = -\frac{1}{\rho}\frac{\partial P}{\partial y} + \frac{\partial}{\partial z}\left(-\overline{v'w'}\right) \tag{2}$$

where $-\overline{u'w'}$ and $-\overline{u'w'}$ are the Reynolds stresses and P is the pressure of the flow.

The Reynolds stresses are modelled in the form:

$$-\overline{u'w'} = \nu_t \frac{\partial u}{\partial z}, \qquad -\overline{v'w'} = \nu_t \frac{\partial v}{\partial z} \tag{3}$$

where ν_t represents the turbulent viscosity.

In order to close the above system of equations, a particular turbulence closure model is required (Launder and Spalding, 1972; Rodi, 1980). For analytical models, the turbulent viscosity is often expressed in the form:

$$\nu_t = \kappa \hat{u}^* f(z) \tag{4}$$

where $\kappa = 0.4$ is von Karman's constant, $\hat{u}^*$ is the maximum bed shear velocity and f(z) is a function of the depth z. For numerical models, the simplest form of ν_t is the following:

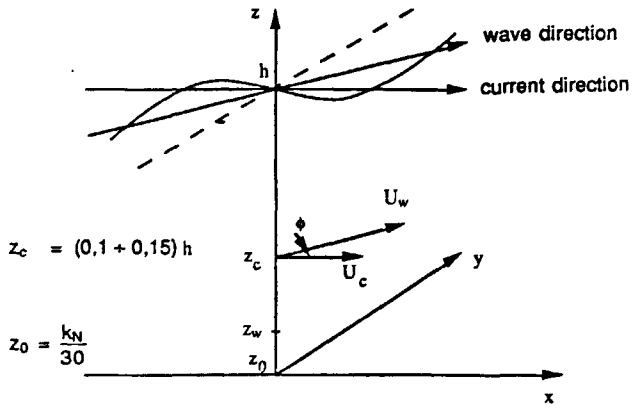

Figure 1

Scheme of the wave-current interaction system.

Schéma du système d'interaction houle-courant.

$$\nu_t = l^2 \left|\frac{\partial u}{\partial z}\right| \tag{5}$$

where *l* is Prandtl's mixing length (Schlichting, 1979).

In general, for the closure problem, one can use an equation for the turbulent kinetic energy K and another for the quantity $K^m L^n$ (for example, the viscous dissipation ε which is proportional to $K^{3/2} L^{-1}$, or the vorticity fluctuation which can be taken as proportional to $K^{1/2} L^{-1}$). Here L represents a macroscale of the turbulent eddies. It should be emphasized that L is equal neither to the integral scale of the flow, nor to Prandtl's mixing length. There exist two approaches to the determination of L. Firstly, L can be empirically determined by the fact that it cannot exceed some fraction of the total spread of the turbulent region and that, close to a wall, it should be proportional to the distance from the wall. These are two boundary conditions for L that will be expressed later. The second approach consists in building up a dynamic equation for L with coefficients that are independent of flow geometry. The turbulence model originally proposed by Lewellen (1977) is a second-order closure model (or a Reynolds stress model). If the turbulence is assumed to be in local equilibrium so that there is no time evolution nor spatial diffusion, one can obtain the algebraic relationships between the Reynolds stresses and the gradients of the mean velocity. Under this local equilibrium approximation, Sheng (1984) and Sheng and Villaret (1989) have found the following form of ν_t:

$$\nu_t = \frac{\sqrt{2}}{4}\sqrt{K}L \tag{6}$$

The turbulent energy K is calculated from Equation (7):

$$\frac{\partial K}{\partial t} = \nu_t\left[\left(\frac{\partial u}{\partial z}\right)^2 + \left(\frac{\partial v}{\partial z}\right)^2\right] - \frac{\nu_t}{L^2}K + 1{,}2\frac{\partial}{\partial z}\left(\nu_t \frac{\partial K}{\partial z}\right) \tag{7}$$

and, for the second approach, L is determined from Equation (8):

$$\frac{\partial L}{\partial t} = 0{,}175\frac{\nu_t}{K}\left[\left(\frac{\partial u}{\partial z}\right)^2 + \left(\frac{\partial v}{\partial z}\right)^2\right]L + 0{,}075\sqrt{2K}$$

$$+ \ 1{,}2\frac{\partial}{\partial z}\left(\nu_t \frac{\partial L}{\partial z}\right) - \frac{0{,}375\sqrt{2}}{\sqrt{K}}\left[\frac{\partial\left(\sqrt{K}L\right)}{\partial z}\right]^2 \qquad (8)$$

The empirical coefficients appear in Equations (7) and (8). Each coefficient was evaluated from a critical flow experiment involving only that coefficient (Lewellen, 1977). It is also noted that the last term in Equation (8) is the additional term in comparison with the classic equation for ε (Rodi, 1980).

The pressure gradients in (1) and (2) are expressed as the sum of the pressure gradient due to the wave and that due to the current, in accordance with the scheme given in Figure 1:

$$-\frac{1}{\rho}\frac{\partial P}{\partial x} = -\frac{1}{\rho}\frac{\partial P_w}{\partial x} - \frac{1}{\rho}\frac{\partial P_c}{\partial x}, \qquad -\frac{1}{\rho}\frac{\partial P}{\partial y} = -\frac{1}{\rho}\frac{\partial P_w}{\partial y} \qquad (9)$$

where P_w is the pressure due to wave and P_c represents the pressure due to current.

At the bottom ($z = z_0$), the boundary conditions in all cases are the following:

$$u = v = 0; \quad \partial K / \partial z = 0;$$
$$L = \alpha z_0 \ \text{ with } \ \alpha = 1.68\kappa = 0.67 \qquad (10)$$

The conditions at the upper limit of the boundary layer depend on each case studied and will be described later.

The above set of equations is discretized using the implicit finite control volume method (Patankar, 1980) on a vertical grid whose step size increases exponentially from bottom to top, thus giving good resolution near the bed where velocity gradients are important. The time step is taken to be constant over the whole period T of the flow. Each discretized equation corresponds to a tridiagonal matrix which can be solved by means of Thomas's algorithm (Roache, 1976). The criterion of convergence is imposed on the velocity calculation: when the absolute error of velocities corresponding to the instant t and t + T is smaller than 10^{-4}, the convergence is obtained.

CASE OF CURRENT ALONE AND WAVE ALONE

Because the goal of this paper is essentially relative to the wave-current interaction, we only present here some principal results for current alone and wave alone.

Current alone

The modelling of a unidirectional steady current is made by putting v = 0 in the above set of equations. At the free surface z = h, the following conditions for u and K are imposed:

$$\partial u / \partial z = 0; \quad \partial K / \partial z = 0 \qquad (11)$$

The scale L can be calculated by two ways:

– either L is directly imposed as a function of z: $L = \alpha z$.

– or L is determined from Equation (8) with the condition $\partial L / \partial z = 0$ at z = h.

The x momentum equation obtained by averaging the depth gives the pressure gradient:

$$-\frac{1}{\rho}\frac{\partial P_c}{\partial x} = \frac{\tau_c}{\rho h} \qquad (12)$$

where τ_c is the bed shear stress of the current.

In reality, these two ways give the same result because the difference of L in the upper region of the flow does not have a considerable effect on the near-bed region. The shear stress τ_c is related to the depth-averaged velocity U_{cm} by the friction coefficient f_c in the following way:

$$\tau_c / \rho = -\overline{u'w'} = \frac{1}{2} f_c U_{cm}^2 \qquad (13)$$

We have run the model for many values of h/z_0 and the Figure 2 shows the variation of f_c in terms of h/z_0 with numerical result for three values.

It is also necessary to note that in the inertial layer near the bed, the energy K and the Reynolds stress $-\overline{u'v'}$ are constant. In order to model this layer where the pressure gradient due to current vanishes, one only has to get the conditions $\partial K / \partial z = 0$, $L = \alpha z$ and $u = U_c$ at the upper limit of the layer $z = z_c$. The value of z_c may be estimated to be equal to (0.10 ÷ 0.15) h (Dyer, 1986).

For a uniform steady flow, the vertical velocity profile is logarithmic and the depth-averaged velocity U_{cm} is obtained at the level $z_{cm} = h/e$.

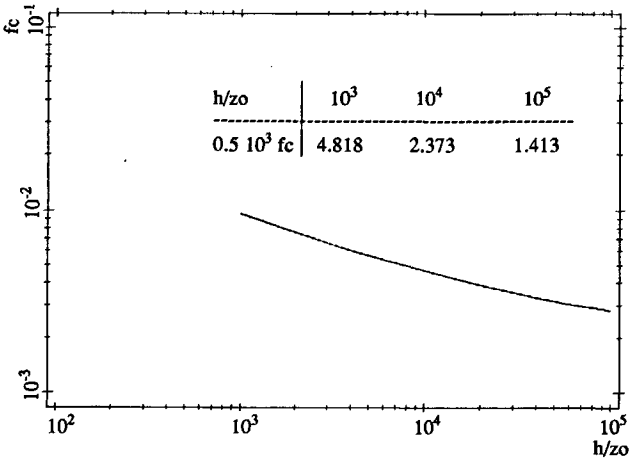

Figure 2

Variation of the friction coefficient f_c of current alone in function of h/z_0.

Variation du coefficient de frottement f_c du courant seul en fonction de h/z_0.

Wave alone

In the case of a unidirectional wave propagating in the x direction, the above set of equations is solved by taking v = 0. The pressure gradient is given by:

$$-\frac{1}{\rho}\frac{\partial P}{\partial x}=\frac{\partial U_w}{\partial t} \qquad (14)$$

where U_w is the wave velocity at the upper limit $z = z_w$ of the wave boundary layer. With regard to the compatibility of the whole study, the value of z_w is taken to be equal to $z_{cm} = h/e$ even though the true value of z_w is much smaller than z_{cm} in reality. For a sinusoidal wave, we have:

$$U_w = \hat{U}_w \sin \omega t \qquad (15)$$

with $\omega = 2\pi/T_w$, T_w being the period of the wave and $\hat{U}_w$ is the maximum velocity.

At $z = z_w$ the boundary conditions are:

$$K = L = 0 \quad \text{and} \quad U = U_w \qquad (16)$$

In investigations of the wave boundary layer, the friction coefficient f_w introduced by Jonsson (1963) is often used:

$$\tau_w / \rho = -\overline{u' w'} = \frac{1}{2} f_w U_w^2 \qquad (17)$$

where $\tau_w = -\rho\overline{u'w'}$ is the maximum shear stress at the bed.

Many empirical and theoretical formulas for f_w exist that depend on the experimental data, and on the analytical or numerical models used. The variation of f_w obtained by the present model in function of A/z_0 (with $A = \hat{U}_w/\omega$) is presented on Figure 3 in comparison with Jonsson's result. A quantitative comparison with experimental data of Jonsson and Carlsen (1976), Sumer *et al.* (1986) and Sleath (1987) can be found in Huynh-Thanh (1990a). Huynh-Thanh and Temperville (1990b, 1990c).

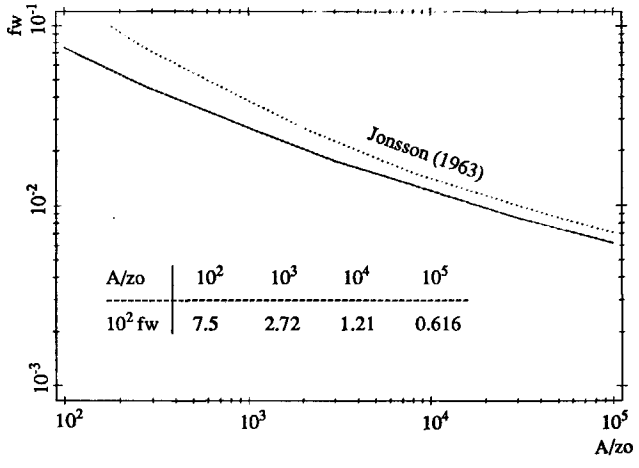

Fig. 3

Variation of the friction coefficient f_w of wave alone in function of A/z_0.

Variation du coefficient de frottement f_w de la houle seule en fonction de A/z_0.

CASE OF WAVE AND CURRENT INTERACTION

The investigation of the boundary layer in wave-current interaction is performed in detail using the complete set of Equations (1) to (10).

Different cases of modelling

We consider here the simplest case in which a sinusoidal wave is superposed on a current. Let U_{cm} be the depth-averaged velocity of the current alone at the level $z_{cm} = 0.368$ h (Yalin, 1977) and U_w be the wave alone orbital velocity. As is well known, a current may be formed by giving either the discharge $Q_c = hU_{cm}$ or the mean free surface slope I_c. From the last quantity, the bed shear stress of the current can be obtained (Yalin, 1977):

$$\tau_c / \rho h = g I_c \qquad (18)$$

and then the pressure gradient of the current is determined from (12).

These two ways of formulation for a current alone suggest two ways of formulating the boundary layer problem under wave-current interaction, as discussed by Van Doorn (1981) and Davies *et al.* (1988): either the discharge Q_c (or the velocity U_{cm}) of the current alone is conserved or the pressure gradient $-\partial P_c / \rho\partial x$ is conserved. For the first way, the mean bed shear stress of the current after interaction will increase in comparison with that of the current alone because of the presence of wave. It follows that the mean pressure gradient of the current must increase. For the second way, the velocity U_{cm} of the current alone will be decreased in order to compensate for the friction generated by the wave, which corresponds to a reduction of the discharge. The last way of modelling was studied by Davies *et al.* (1988).

In this paper, we propose to analyse the problem based on the conservation of the discharge $Q_c = hU_{cm}$ of the current alone. Results of experiments concerning the boundary layer in wave-current interaction cited in introduction show that when the wave is superposed on the current, the zone close to the bed of the current alone is affected by the turbulence due to the wave; in consequence the velocity profile has to be changed. Hence, it may be that the velocity U_{cm} of the current alone is different from the velocity U_{cm1} of the current after interaction at the same level $z_{cm} = 0.368$ h. Nevertheless, the change of mean velocity profiles is such that the discharge Q_c must be constant. The possible difference between U_{cm} and U_{cm1} is expected to depend on various parameters of wave, current, bed roughess and angle of interaction. In reality, if the velocity U_{cm1} is given, there is no difficulty for modelling: this value will be directly introduced in the model. On the other hand, the value of U_{cm} may be used at first approximation. In order to verify the validity of this approximation, we propose a modelling process as follows:

– First stage: we take $U_{cm1} = U_{cm}$ where U_{cm} was obtained for a current alone calculated up to the free surface. The upper limit is put at the level $z_{cm} = 0.368$ h with the conditions:

$$\partial K / \partial z = 0; \quad L = \alpha z;$$
$$u = U_{cm1} + U_w \cos\phi; \quad v = U_w \sin\phi \qquad (19)$$

and with the pressure gradient of the initial current determined by (12). The model run gives the mean shear stress τ_m.

– Second stage: from the value of τ_m obtained, we calculate the pressure gradient of the current after interaction by:

$$-\frac{1}{\rho}\frac{\partial P_c}{\partial x} = \frac{\tau_m}{\rho h} \qquad (20)$$

Now, the upper limit is treated at the free surface z = h with the pressure gradient (20) and with the conditions:

$$\partial u / \partial z = 0; \quad \partial v / \partial z = 0; \quad \partial K / \partial z = 0; \quad L = \alpha z \qquad (21)$$

From the mean velocity profile obtained, we calculate the discharge Q_{cl}. If Q_{cl} is different from Q_c, another value of the pressure gradient will be chosen for the next run, beginning at the second stage. The process may be continued until the calculated discharge is equal to Q_c.

For illustration purpose, we shall present some numerical results with the following parameters:

Initial current: U_{cm} = 39.25 cm/s and 392.5 cm/s;

Wave: $\hat{U}_w$ = 157 cm/s and 78.5 cm/s; T_w = 8 s;

Bed roughness: z_0 = 0.2 cm;

Water depth: h = 20 m;

Angle of interaction: $\phi = 0°, 45°, 90°$.

These values are combined so that we obtain:

$A/z_0 = 10^3$; $z_0/h = 10^{-4}$; $U_{cm}/\hat{U}_w = 0.25$ and 5.

Table 1 presents results for some model runs. The relative errors are defined by:

$$\text{Err 1} = |\tau_m - \tau_{m1}| / \tau_m$$
$$\text{Err 2} = |Q_c - Q_{c1}| / Q_c$$

with τ_{m1} being the mean bed shear stress corresponding to every run in each example.

It can be seen from Table 1 that, in order to obtain the same discharge Q_c, it is necessary to use a pressure gradient greater than that calculated with the mean bed shear stress τ_m (the maximum difference is inferior to 5 %). For all the cases of calculation, a maximum relative error less than 1 % is found between the discharge Q_{cl} obtained from the second run and the exact discharge Q_c obtained from the initial current. The maximum relative error between the mean bed shear stresses τ_m obtained from the calculation at z = z_{cm} and the exact mean bed shear stress τ_{m1} is less than 5 %.

Hence, if an error in the order of 5 % on the discharge as well as on the mean bed shear stress of current after interaction is accepted for practical purposes, one can use the value of U_{cm} determined from the current alone for the calculation in the case wave-current interaction.

Figures 4, 5 and 6 present the mean profiles of velocity, kinetic energy and turbulent viscosity of the current before and after interaction. The departure of the calculated profile of current alone from the straight line which represents the logarithmic law is due to the condition $\partial u / \partial z = 0$ applied at the free surface in the model.

From the above analysis, we distinguish the following cases of modelling, according to the position of the upper limit of the boundary layer z = z_1:

– **Case 1**: the upper limit is treated at the mean depth $z_1 = z_{cm}$. At this level, the current velocity is taken to be equal to that of the current alone U_{cm}, and the pressure gradient due to current is determined from the current alone. The validity of this approximation was verified as above.

– **Case 2**: the upper limit is treated at the free surface z_1 = h. The pressure gradient due to current must be determined with the mean shear stress of the current after interaction, which is difficult to estimate *a priori*, particularly for small values of the ratio $U_{cm}/\hat{U}_w$.

Another case of modelling is envisaged, arising from the fact that the boundary layer can be investigated as an inertial layer, from which we have:

– **Case 3**: the upper limit is chosen at the top of the inertial layer $z_1 = z_c = (0.10 \div 0.15)$ h. In this case, the pressure gra-

Table 1

Ex.	$U_{cm}/\hat{U}_w$	τ_c/ρ	Q_c	$\phi°$	τ_m/ρ	Run	$-\frac{1}{\rho}\frac{\partial P_c}{\partial x}$	τ_{m1}/ρ	Q_{c1}	Err1	Err2
		m^2/s^2	m^2/s		m^2/s^2	n°	m/s^2	m^2/s^2	m^2/s	%	%
1	0.25	3.66	7.64	0	15.2	1	0.00760	15.8	7.51	4.0	1.7
						2	0.00785	16.0	7.66	5.2	0.3
2	-	-	-	45	13.7	1	0.00685	13.8	7.47	0.7	2.2
						2	0.00710	14.3	7.67	4.4	0.4
3	-	-	-	90	11.8	1	0.00590	11.9	7.38	0.8	3.4
						2	0.00650	12.3	7.68	4.2	0.5
4	5	366	77.8	0	381	1	0.19100	368	76.4	3.4	1.8
						2	0.19700	380	77.6	0.3	0.3
5	-	-	-	45	378	1	0.18900	364	76.4	3.5	1.8
						2	0.19500	376	77.6	0.4	0.3
6	-	-	-	90	373	1	0.18700	360	76.3	3.7	1.9
						2	0.19400	373	77.8	0.1	0.0

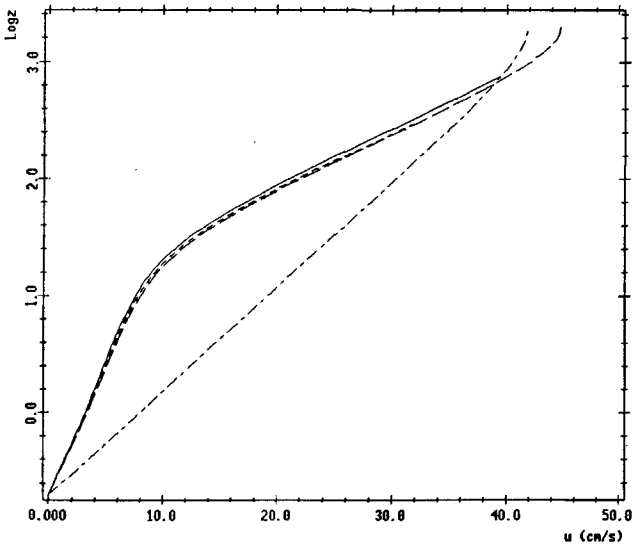

Figure 4

Mean velocity profiles of current (U_{cm} = 39.25 cm/s, $\hat{U}_w$ = 157 cm/s, T_w = 8 s, z_0 = 0.2 cm, h = 20 m, ϕ = 0°).
Current alone — *with z_1 = h*
Current after interaction — *with $z_1 = z_c$ = 0.15 h,* — *with $z_1 = z_{cm}$ = 0.368 h,* — *with z = h.*

Profils de vitesse moyenne du courant.
Courant seul — avec z_1 = h
Courant après l'interaction — avec $z_1 = z_c$ = 0,15 h, — avec $z_1 = z_{cm}$ = 0,368 h. — avec z = h.

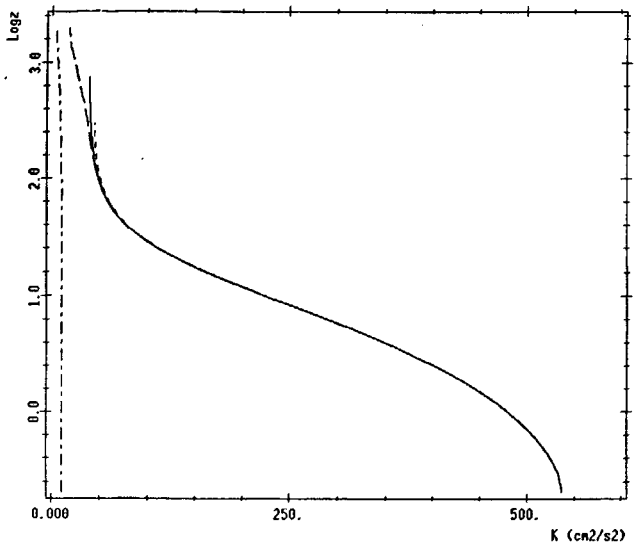

Figure 5

Mean kinetic energy profiles of current. See Fig. 4 for symbols.

Profils de l'énergie cinétique moyenne du courant. Voir Fig. 4 pour les symboles.

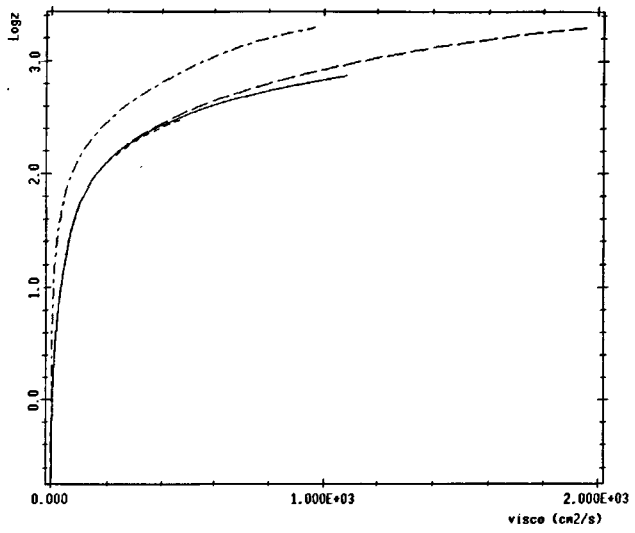

Figure 6

Mean turbulent viscosity profiles of current. See Fig. 4 for symbols.

Profils de la viscosité turbulente moyenne du courant. Voir Fig. 4 pour les symboles.

dient associated with the current vanishes but it is necessary to know the exact value of the mean velocity of current ater interaction at this level. This unknown value is very different from the velocity of current alone at this level, particularly for the case in which current is dominated by wave.

Figures 4, 5 and 6 also illustrate the third case of modelling in which the velocity of current U_{cl} at $z = z_c = 0.15$ h is chosen to be equal to the value obtained from the mean velocity profile of current after interaction in case 2. Note that the relative difference $(U_c - U_{cl})/U_c$ is equal to 10 %, being the current alone velocity at $z = z_c$.

Very good agreement between results from the three cases of calculation shows that they are physically equivalent, provided, of course, that they are well formulated. However, from a numerical viewpoint, case 2 requires much more calculation time than the others because of the Neumann conditions at the free surface and the vertical grid extended on the total water depth; case 3 takes the least CPU time due to the Dirichlet conditions at $z = z_c$ as well as the grid that occupies only a small portion of water depth. Our numerical experiments give a ratio equal to 10 for CPU time between case 2 and case 1 and a ratio equal to 0.5 between case 3 and case 1. Regarding advantages, disadvantages and precision of these cases, we see that case 1 is most appropriate to run the model. The results presented in the following were obtained with this case of modelling. The model validity was verified by the quantitative comparison with the experimental data of Van Doorn (1981) (see for example Huynh-Thanh and Temperville, 1990b).

Mean and maximum bed shear stress for a simple velocity signal

One of the aims of a wave-current interaction model is to supply information on the variation of mean and maximum bed shear stress for different parameters of wave, current, bed roughness and angle of interaction. Here a simple signal means that a sinusoidal wave is superposed on a current. The model was run for the following combinations of parameters which cover a wide range of real cases:

$\phi = 0°, 15°, 30°, 45°, 60°, 75°, 90°$;
$z_0/h = 10^{-5}, 10^{-4}, 10^{-3}$;
$A/z_0 = 10^2, 10^3, 10^4, 10^5$
$U_{cm}/\hat{U}_w = 0.25, 0.5, 0.75, 1, 1.25, 1.5, 1.75, 2, 2.5, 3, 3.5, 4, 5, 7, 10.$

For reasons of space, only some results are presented here. Plots for the dimensionless mean bed shear stress $\tau_m / (\tau_c + \tau_w)$ and the dimensionless maximum bed shear stress $\tau_{max} / (\tau_c + \tau_w)$ over a wave period are shown in Figure 7 in terms of $\tau_c / (\tau_c + \tau_w)$. Values of the bed shear stress τ_c of current alone and the bed shear stress τ_w of wave alone can be determined from the curves in Figures 2 and 3.

Three remarks are called for concerning the variables chosen: firstly, $\tau_c / (\tau_c + \tau_w)$ varies only from 0 (wave alone) to 1 (current alone); secondly, the linear superposition of a wave on a current corresponds to a linear variation from 0 to 1 for $\tau_m/(\tau_c + \tau_w)$; and thirdly, for $\tau_{max}/(\tau_c + \tau_w)$, the linear superposition gives a constant variation equal to 1 for $f = 0°$ and a parabolic variation equal to $\sqrt{\tau_c^2 + \tau_w^2} / (\tau_c + \tau_w)$ for $= 90°$.

One of advantages of this graphic representation method is that it shows directly the nonlinearity nature of the problem. It is proposed by Soulsby *et al.* (1992) and utilized for the intercomparison between different models of wave-current interaction boundary layer, including the present, in the framework of the european program MAST 1. It can be seen that the nonlinear enhancement increases τ_{max} by up to 60 % and τ_m by up to 15 % for colinear flows. This nonlinearity decreases when f increases. For the same values of ϕ and z_0/h, the maximum values of τ_{max} and τ_m reduce when A/z_0 decreases. The variation of τ_{max} for $\phi = 90°$ is interesting: τ_{max} is larger than the value obtained without nonlinear superposition $\sqrt{\tau_c^2 + \tau_w^2}$ but smaller than the value of $(\tau_c + \tau_w)$.

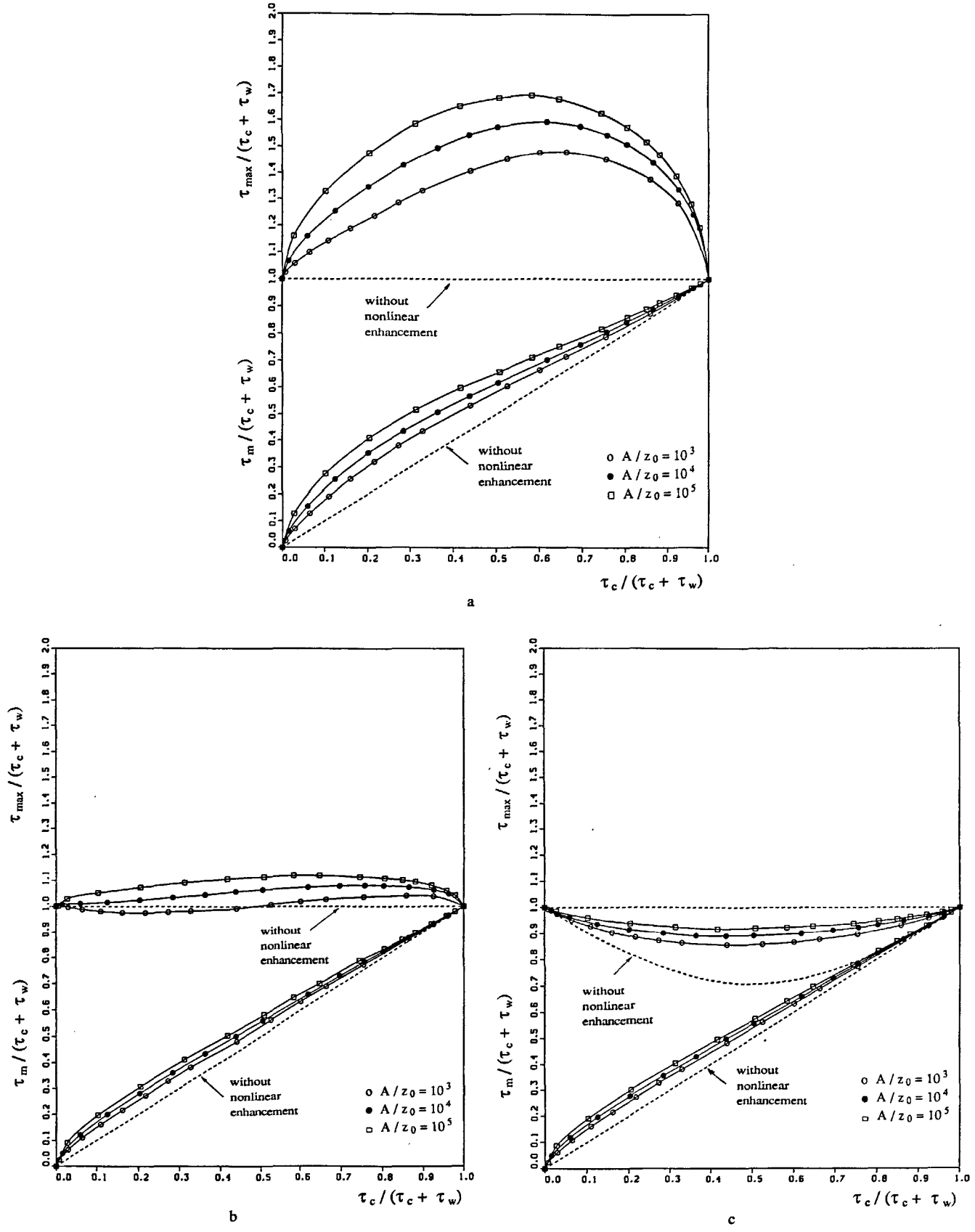

Figure 7

Variation of mean and maximum bed shear stresses in function of A/z_0 for $z_0/h = 10^{-5}$ and many values of $U_{cm}/\hat{U}_w$
a) with $\phi = 0°$; b) with $\phi = 75°$; c) with $\phi = 90°$.

Variation des contraintes de cisaillement moyenne et maximale en fonction de A/z_0 pour $z_0/h = 10^{-5}$ et plusieurs valeurs de $U_{cm}/\hat{U}_w$
a) avec $\phi = 0°$; b) avec $\phi = 75°$; c) avec $\phi = 90°$.

Table 2

N°	b	p	q	maxerr	a	n	m	maxerr
phi = 0 degree								
1	0.3891	-0.3877	1.6000	3.5	1.4197	1.0601	0.6000	2.4
2	0.5191	-0.4381	1.6000	3.8	1.6460	0.9207	0.6000	3.5
3	0.6797	-0.4745	1.6000	1.3	1.7865	0.7801	0.6000	4.5
4	0.2404	-0.4706	1.6000	1.7	1.2284	1.0478	0.6000	1.7
5	0.4067	-0.4697	1.6000	2.2	1.4496	0.9335	0.6000	3.0
6	0.5986	-0.4988	1.6000	1.2	1.6441	0.7828	0.6000	4.0
7	0.3163	-0.4977	1.6000	0.5	1.2176	0.9172	0.6000	2.0
8	0.5317	-0.5173	1.6000	0.9	1.3992	0.7230	0.6000	2.7
phi = 15 degree								
1	0.3575	-0.4042	1.6000	1.0	1.3759	1.1057	0.6000	3.6
2	0.4920	-0.4493	1.6000	0.6	1.5933	0.9340	0.6000	2.9
3	0.6421	-0.4860	1.6000	1.4	1.7186	0.7828	0.6000	4.5
4	0.2300	-0.4750	1.6000	1.7	1.1801	1.0630	0.6000	1.8
5	0.3869	-0.4722	1.6000	1.0	1.3916	0.9400	0.6000	2.9
6	0.5706	-0.5052	1.6000	1.6	1.5963	0.7960	0.6000	4.3
7	0.3007	-0.5088	1.6000	0.8	1.1596	0.9154	0.6000	2.0
8	0.5073	-0.5248	1.6000	0.9	1.3451	0.7286	0.6000	2.8
phi = 30 degree								
1	0.3198	-0.4136	1.6000	1.0	1.2105	1.1498	0.6000	3.3
2	0.4306	-0.4668	1.6000	1.8	1.3966	0.9449	0.6000	2.7
3	0.5655	-0.5001	1.6000	1.3	1.5143	0.7854	0.6000	4.2
4	0.2000	-0.5041	1.6000	2.0	1.0372	1.1103	0.6000	1.8
5	0.3338	-0.4996	1.6000	1.3	1.2238	0.9629	0.6000	2.8
6	0.5059	-0.5180	1.6000	1.2	1.4184	0.8256	0.6000	4.5
7	0.2612	-0.5379	1.6000	1.7	1.0265	0.9876	0.6000	2.5
8	0.4475	-0.5419	1.6000	0.9	1.1865	0.7455	0.6000	2.9
phi = 45 degree								
1	0.2239	-0.5324	1.6000	0.9	0.9467	1.2323	0.6000	3.0
2	0.3441	-0.5013	1.6000	5.0	1.1058	0.9826	0.6000	2.3
3	0.4663	-0.5168	1.6000	1.8	1.2258	0.8211	0.6000	3.9
4	0.1659	-0.5371	1.6000	2.0	0.8088	1.2124	0.6000	1.5
5	0.2707	-0.5352	1.6000	1.4	0.9585	1.0088	0.6000	2.5
6	0.4154	-0.5397	1.6000	1.2	1.1294	0.8530	0.6000	4.0
7	0.2130	-0.5778	1.6000	2.3	0.8006	1.0640	0.6000	2.3
8	0.3715	-0.5653	1.6000	1.6	0.9332	0.7749	0.6000	2.8
phi = 60 degree								
1	0.1845	-0.5548	1.6000	0.9	0.6064	1.4753	0.6000	2.6
2	0.2707	-0.5411	1.6000	1.0	0.7470	1.1243	0.6000	1.4
3	0.3687	-0.5471	1.6000	1.2	0.8127	0.8393	0.6000	2.9
4	0.1285	-0.5939	1.6000	3.0	0.5074	1.5270	0.6000	0.8
5	0.2114	-0.5792	1.6000	1.7	0.6322	1.1885	0.6000	2.1
6	0.3300	-0.5657	1.6000	1.2	0.7509	0.9104	0.6000	3.2
7	0.1680	-0.6265	1.6000	3.7	0.5027	1.2967	0.6000	1.8
8	0.2927	-0.5921	1.6000	1.2	0.6001	0.8366	0.6000	2.5
phi = 75 degree								
1	0.1588	-0.5748	1.6000	0.9	0.1840	2.7000	0.6000	1.0
2	0.2212	-0.5767	1.6000	1.6	0.3279	1.8529	0.6000	1.8
3	0.2978	-0.5739	1.6000	1.8	0.3487	0.9836	0.6000	1.9
4	0.1041	-0.6394	1.6000	4.0	0.0956	4.8000	0.6000	0.5
5	0.1699	-0.6182	1.6000	2.0	0.2824	2.7058	0.6000	0.5
6	0.2669	-0.5909	1.6000	1.1	0.3079	1.1702	0.6000	2.0
7	0.1394	-0.6520	1.6000	2.9	0.1257	3.0000	0.6000	1.9
8	0.2371	-0.6212	1.6000	1.0	0.2125	1.2530	0.6000	1.8
phi = 90 degree								
1	0.1594	-0.5658	1.6000	0.9	-0.3016	0.5228	0.6000	1.6
2	0.2056	-0.5923	1.6000	0.6	-0.2247	0.4977	0.6000	2.2
3	0.2711	-0.5883	1.6000	1.7	-0.1758	0.5631	0.6000	1.0
4	0.0927	-0.6699	1.6000	5.0	-0.3429	0.5265	0.6000	2.8
5	0.1540	-0.6350	1.6000	2.0	-0.2820	0.5277	0.6000	2.1
6	0.2448	-0.5989	1.6000	1.0	-0.2153	0.5564	0.6000	1.2
7	0.1264	-0.6669	1.6000	3.7	-0.3399	0.5771	0.6000	2.0
8	0.2146	-0.6313	1.6000	1.1	-0.2501	0.5212	0.6000	2.1

Note

z_0/h	10^{-5}			10^{-4}			10^{-3}	
A/z_0	10^3	10^4	10^5	10^2	10^3	10^4	10^2	10^3
N°	1	2	3	4	5	6	7	8

For $\phi = 75°$, some curves of τ_{max} present an "oscillation" about the linear value $(\tau_c + \tau_w)$, as seen on Figure 7b. For practical purpose, it can be considered that these values of τ_{max} are equal to $(\tau_c + \tau_w)$, because the relative error between the exact values of τ_{max} and those of $(\tau_c + \tau_w)$ is smaller than 5 %.

It is important to parameterize the mean and maximum bed shear stress to facilitate the incorporation of results in a coastal morphodynamic model. For this, Soulsby *et al.* (1992) have suggested two following algebraic functions:

$$Y_{max} = 1 + aX^m (1 - X)^n;$$

$$Y_m = X [1 + bX^p (1 - X)^q] \quad (22)$$

with $Y_{max} \equiv \tau_{max} / (\tau_c + \tau_w)$;

$$Y_m \equiv \tau_m / (\tau_c + \tau_w); \quad X \equiv \tau_c / (\tau_c + \tau_w) \quad (23)$$

and the coefficients a, m, n, b, p, q are functions of z_0/h, A/z_0 and ϕ.

The values of these coefficients obtained with the present model are given in Table 2, with the estimation of maximum error (maxerr) between the exact and fitted curves.

SUMMARY AND CONCLUSION

In this paper, we have analysed different cases of modelling for the turbulent boundary layer due to wave-current interaction. The case which is suitable for the modelling is that in which the calculation is carried out at the mean-depth $z = z_{cm} = h/e$. For a simple combination of a sinusoidal wave and a current, the model results present clearly the non-linearity effect of the interaction. The model will be applied to a more complex velocity signal in the MAST 2 programme.

Acknowledgements

This work was carried out as part of the G6 Coastal Morphodynamics programme. It was funded jointly by the GDR Manche French programme and the Commission of the European Communities, Directorate-General for Science Research and Development, under contract n° MAST-CT-0035-C.

REFERENCES

Davies A. G., R. L. Soulsbyand and H. L. King (1988). A numerical model of the combined wave and current bottom boundary layer. *J. Geophys. Res.* **93** (C1), 491-508.

Davies A. G. (1990). A model of the vertical structure of the wave and current bottom boundary layer. In *Modeling Marine systems.* CRC Press, 263-297.

Dyer K. R. (1986). *Coastal and estuarine sediment dynamics.* Eds. Wiley-Interscience.

Huynh-Thanh S. (1990a). Etude numérique de la couche limite turbulente oscillatoire générée par l'interaction houle-courant en zone côtière. Thèse de Doctorat. Institut National Polytechnique de Grenoble.

Huynh-Thanh S. and A. Temperville (1990b). A numerical model of the rough turbulent boundary layer in combined wave and current interaction. In *Sand Transport in Rivers, Estuaries and the Sea.* Balkema Publ. 93-100.

Huynh-Thanh S. and A. Temperville (1990c). A numerical model of the wave-current turbulent boundary layer over sea beds. *Proc. 22nd Conf. Coastal Eng.* Delft, Hollands, 1, chap. 65, 853-866.

Jonsson I. G. (1963). Measurements in the turbulent wave boundary layer. *Proc. 10th Congr. IAHR,* 85-92.

Jonsson I. G. and N. A. Carlsen (1976). Experimental and theoretical investigations in an oscillatory turbulent boundary layer. *J. Hydraul. Res.* 14, **1**, 45-60.

Kamphuis J. W. (1975). Friction factors under oscillatory waves. *J. Waterw. Harbors Coastal Eng. Div.* 101 (WW 2), 135-144.

Launder B. E. and D. B. Spalding (1972). *Mathematical models of turbulence.* Academic Press.

Lewellen W. S. (1977). Use of invariant modeling. In *Handbook of turbulence.* Plenum Publishing Corp., Vol. 1.

Patankar S. (1980). *Numerical heat transfer and fluid flows.* McGraw Hill Book Co.

Roache P. J. (1976). *Computational fluid dynamics.* Eds. Hermosa Publishers.

Rodi W. (1980). *Turbulence models and their applications in hydraulics.* IAHR, Delft, The Netherlands.

Sheng Y. P. (1984). A turbulent transport model of coastal processses. *Proc. 19th Conf. Coastal Eng.* 2380-2396.

Sheng Y. P. and C. Villaret (1989). Modeling the effect of suspended sediment stratification on bottom exchange processes. *J. Geophys. Res.* 94 (C10), 14, 429-14, 444.

Sleath J. F. A. (1987). Turbulence oscillatory flow over rough beds. *J. Fluid Mech.* 182, 369-409.

Soulsby R. L. *et al.* (1993). Wave-current interaction within and outside the bottom boundary layer. *Coastal Engineering* 21, 41-69.

Sumer B. M., B. L. Jensen and J. Fredsoe (1986). Turbulence in oscillatory boundary layers. In *Advances in Turbulences* 556-567.

Van Doorn Th. (1981). Experimental investigation of near-bottom velocities in water waves without and with a current. *Delft Hydraul. Lab. Rep.* M1423. Part 1.

Yalin M. S. (1977). *Mechanics of sediment transport.* Pergamon Press.